THE ASTROPHYSICAL JOURNAL, 460:L73–L76, 1996 March 20

RECONNECTION-DRIVEN CURRENT FILAMENTATION IN SOLAR ARCADES

JUDITH T. KARPEN AND SPIRO K. ANTIOCHOS
Code 7670, E. O. Hulburt Center for Space Research, Naval Research Laboratory, Washington, DC 20375-5352
AND
C. RICHARD DEVORE
Code 6440, Laboratory for Computational Physics and Fluid Dynamics, Naval Research Laboratory, Washington, DC 20375-5344
Received 1995 October 16; accepted 1996 January 10

ABSTRACT

We present numerical simulations of the interaction between two bipoles through magnetic reconnection in the lower solar atmosphere, a process believed to be the origin of many manifestations of solar activity. The present work differs from previous studies in that the field is sheared asymmetrically and that the bipoles have markedly unequal field strengths. Our key discovery is that, under such common circumstances, reconnection leads to an apparently random distribution of shear in the magnetic field, resulting in numerous current sheets throughout the volume occupied by the reconnected field lines. To our knowledge, this is the first example of a numerical simulation yielding current sheets over a large but well-defined volume of the corona, resembling a coronal loop in profile. In this Letter, we demonstrate this process of *reconnection-driven current filamentation* and discuss ramifications for coronal heating and structure.

Subject headings: methods: numerical — MHD — plasmas — Sun: magnetic fields

1. INTRODUCTION

The high Reynolds number of the solar corona ($\geq 10^{10}$) indicates the enormous disparity between the large spatial scales of photospheric motions, which inject energy into the magnetic field, and the small characteristic scales of resistive or viscous dissipation, which yield heating. Hence, a crucial problem in understanding solar activity in general, and coronal heating in particular, is finding a mechanism that can transfer the input energy to the dissipation scales efficiently. This must be accomplished by forming internal boundary layers, such as electric current sheets in direct current (DC) heating models or resonance layers in wave heating models. Most coronal heating studies have investigated mechanisms for developing the required fine structure under the constraint of initially continuous magnetic fields and flows (e.g., van Ballegooijen 1986; Mikić, Barnes, & Schnack 1988; Karpen, Antiochos, & DeVore 1991; Parker 1993)—for example, through Kelvin-Helmholtz instability of intergranular flows (Karpen et al. 1993). However, this process would yield heating distributed approximately uniformly throughout the corona, and hence could not account for the well-defined dimensions and lifetimes of observed coronal loops (e.g., Klimchuk 1995).

Because current sheets and magnetic reconnection develop readily in multipolar magnetic fields, due to the inevitable presence of separatrix surfaces and null points (Syrovatskii 1971; Syrovatskii 1981; Zwingmann, Schindler, & Birn 1985; Antiochos et al. 1994), we have argued that the multipolarity of the photospheric field is a crucial ingredient of solar activity (Antiochos 1987; Antiochos 1990; Karpen, Antiochos, & DeVore 1995, hereafter KAD). Compelling observational evidence also supports this contention. Chromospheric eruptions, a collection of highly dynamic events including spicules, surges, sprays, and the high-resolution telescopic spectrometer (HRTS) explosive events, are observed to accompany flux cancellation, as well as merging at the edges of extensive, magnetically strong features such as sunspots and the supergranular network (Rust 1968; Blake & Sturrock 1985; Dere et al. 1991). Even relatively quiescent structures such as X-ray–emitting coronal loops and bright points exhibit clear correlations with mixed polarity regions at their footpoints (Harvey et al. 1994a, b; Moses et al. 1994; Priest, Parnell, & Martin 1994; Falconer et al. 1995). The underlying physical feature unifying these diverse phenomena apparently is the relative motion of flux systems in a multipolar photospheric region.

We propose that a single process—magnetic reconnection in multipolar fields—accounts for both chromospheric dynamics and the heating in complex field regions such as the network and active regions. Previously, we simulated the interaction and reconnection of two identical bipoles driven by symmetric footpoint shearing (KAD), which reproduced the rapid dynamic behavior of chromospheric eruptions but created only two current sheets (one along each separatrix surface) lasting under 1000 s. Therefore, this symmetric model could not account for the long-duration, spatially extended heating of coronal loops. In this Letter, however, we report an exciting new result: if the initial multipolar field is asymmetric, as is generally expected, then footpoint shearing of this configuration leads to the formation of many current sheets over a large but well-defined volume, perhaps explaining the heated structures visible as coronal loops.

2. THE NUMERICAL MODEL

The calculations were performed with MAG25D, our compressible MHD code which uses two two-dimensional flux-corrected transport modules to solve the convective and inductive portions of the equations in 2.5 dimensional (translationally invariant three-dimensional) Cartesian coordinates (DeVore 1991). A more detailed description of the numerical method, initialization, and boundary conditions is given by KAD, with minor changes specific to the asymmetric case to be described in a subsequent paper. The initial magnetic field, shown in Figure 1, is potential with a null line (i.e., a

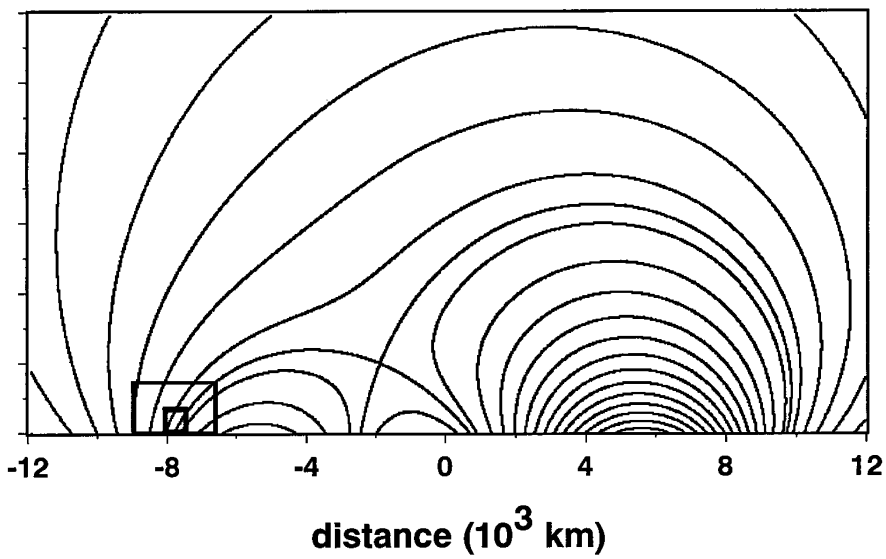

FIG. 1.—Initial magnetic field lines in the computational plane. The spatial distribution of the shearing force is outlined around the footpoint of the leftmost separatrix: the outer box shows the full extent of the applied body force, while the inner box shows the area of maximum (constant) force.

two-dimensional X-point) approximately 2000 km above the photosphere (i.e., the bottom boundary). It is evident from Figure 1 that the field topology contains four distinct flux systems: the left, middle, and right arcades each corresponding to one of the three photospheric neutral lines, and an overlying flux system. Because of the asymmetry deliberately built into the system, the left arcade is significantly smaller than the right arcade. Here x is the vertical coordinate and y the coordinate parallel to the solar surface, while z is the translationally symmetric direction (pointing into the x-y plane). The form of the initial magnetic vector potential along the source surface is given by

$$A_z(x = -b, y) \propto \begin{cases} y^2[1 - (y/a)^2]^2, & 0 \le y \le a, \\ Ky^2[1 - (y/a)^2]^2, & -a \le y < 0, \\ 0, & |y| > a, \end{cases} \quad (1)$$

where the horizontal scale $a = 10^9$ cm, the vertical offset $b = 2.4 \times 10^8$ cm, and the arbitrary asymmetry factor $K = 2$. The initial vector potential in the interior of the computational box is determined by integration of Laplace's equation over the upper half-plane, with equation (1) as the lower boundary condition and $A_z = 0$ at infinity. Hence,

$$A_z(x, y) \propto \frac{x + b}{\pi} \int_{-a}^{a} \frac{\xi^2[1 - (\xi/a)^2]^2}{(\xi - y)^2 + (x + b)^2}\, d\xi. \quad (2)$$

The field was sheared by imposing a local, time-dependent body force deep in the chromosphere, at the base of the outer separatrix between the left arcade and the overlying flux (see Fig. 1 for location). After the shearing was discontinued at 1000 s, the system was allowed to relax for an additional 1000 s. Note that both the field and the shear are asymmetric.

An important feature of the model is our use of a solar-like atmosphere with a chromosphere several scale heights deep, a thin transition region with a scale height of 500 km, and a larger, low-β corona (see KAD). A fixed nonuniform grid in both directions accommodates both the plasma β variations and the structural evolution near the initial null line. By modeling, as closely as possible, the reconnection process under actual solar conditions, we have resolved the controversy about the existence of "fast reconnection" as applied to closed fields on the Sun (see KAD). Unlike previous simulations aimed at comparing the idealized Sweet-Parker (Sweet 1958; Parker 1963) and Petschek (1964) scenarios, the reconnection in our simulation is insensitive to boundary conditions because the reconnection jets are diverted by the overlying and underlying field well before reaching the computational boundaries. By including a thick chromosphere, we guarantee that all flows slow and eventually stop as they move down the field lines, which obviously occurs on the Sun. Furthermore, we drive the system solely through photospheric motions far from the null line, again motivated by the solar context. The inclusion of compressibility and the hydrostatic solar atmosphere also ensures that we do not neglect pressure gradients and other bulk plasma effects, which are crucial in determining the magnetic topology at the ends of the current sheet, as well as the distinct plasma properties in the magnetic islands.

3. RESULTS AND DISCUSSION

The magnetic field evolves through successive stages of current-sheet formation and reconnection before relaxing to a final quasi-static state. Because the shear is concentrated around the footpoint of the leftmost separatrix, only the overlying flux and the left arcade acquire shear initially. As the shear component of the magnetic field, B_z, propagates from the footpoints, current sheets form at the separatrices due to the discontinuities in B_z between neighboring flux systems. The increased magnetic pressure due to the shear in the left arcade causes it to expand against the unsheared right arcade. Consequently, the X-point deforms into an approximately vertical current sheet with two Y-type cusps at each end. The sheet continues to elongate vertically until it becomes unstable and forms multiple reconnection regions, similar to the symmetric case (see KAD, videotape sequence 4). During the peak reconnection phase (600–950 s), one or more magnetic islands form along the current sheet, rise or fall toward one end of the sheet, and ultimately reconnect with the overlying or underly-

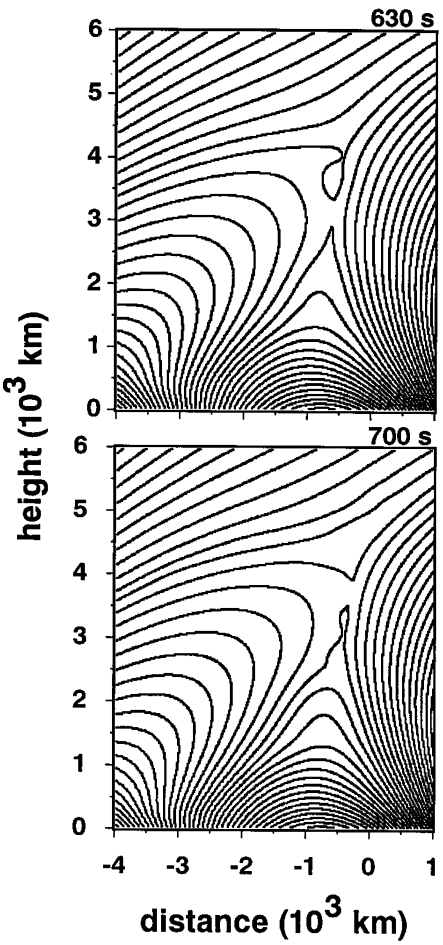

FIG. 2.—Field lines in the vicinity of the reconnecting current sheet at two selected times during the peak reconnection phase, as marked. The field lines are plotted at equal intervals of vector potential. Note that the islands form asymmetrically with one end pinching off before the other, thereby determining the subsequent direction of travel. The island forming at 630 s will rise, therefore, while the one forming at 700 s will fall.

ing field (Fig. 2). The vertical current sheet shrinks steadily through reconnection, temporarily resuming a distorted configuration with an X-point at ~3500 km around 1050 s. The system apparently overshoots its final equilibrium, however, because a roughly horizontal current sheet then forms and becomes unstable at ~1140 s, when it is comparable to the maximum extent of the vertical sheet. The unstable horizontal sheet does not develop a quasi-equilibrium with a single magnetic island, as occurred in the symmetric case. Instead, a transient series of magnetic islands develops, analogous to the evolution of the vertical sheet. Each island is expelled toward the left or right terminus of the sheet, finally reconnecting with the adjacent field. By 1200 s the sheet has shrunk to another X-point at ~2800 km, roughly 1750 km higher and farther to the right than the original location. The system oscillates briefly and reaches a quasi-static state by ~1300 s, after which little change is observed through the end of the run at 2000 s.

We find one crucial feature common to both symmetric and asymmetric cases, thus suggesting its universality in generalized three-dimensional topologies with nulls: the X-point always deforms into a current sheet bounded by two Y-points, as predicted by Syrovatskii (1971, 1981), rather than developing into a tiny diffusion region as required for the Petschek reconnection.

The most exciting and potentially far-reaching discovery drawn from our asymmetric simulation is that the random nature of the reconnection process creates a distribution of current sheets throughout the region occupied by reconnected field lines. This process of *reconnection-driven current filamentation* (RDCF) produces a wide band of currents surrounding the separatrix surfaces, as shown in Figure 3 (Plate L11). To our knowledge, this is the first example of a numerical simulation yielding current sheets over a large but well-defined volume of the corona, resembling a coronal loop in profile. The rebound phenomenon between ~1050 and 1300 s, described above, reprocesses a small amount of flux through the horizontal current sheet and further broadens the region affected by RDCF (see Fig. 3). Note, however, that the strong currents deep in the interior of the left arcade are due to the proximity of the shear force and not to RDCF.

The key to the origin of RDCF is that *the shear acquired by each reconnected field line depends on its reconnection site*. Unlike the symmetric sheared system (KAD) or the compressive two-dimensional models (e.g., Shibata, Nozawa, & Matsumoto 1992; Rickard & Priest 1994), in which the reconnected field lines must end up without shear, the reconnected field lines in a more realistic (asymmetric) system retain finite shears whose magnitudes are determined by their footpoint displacements. Although our system has translational symmetry, it is easiest to understand RDCF by focusing on the reconnection of individual field lines. As the simplest example, we examine the reconnection at a single point somewhere along the vertical current sheet, involving a particular unsheared right-arcade field line. Along the sheet, this line adjoins a continuum of sheared left-arcade field lines with which it can reconnect, each with different footpoint positions. The height of the reconnection point determines which sheared field line reconnects with the representative unsheared line, thus prescribing the footpoint displacements of the corresponding postreconnection field lines. Therefore, the amount of shear remaining after reconnection depends crucially on which two field lines reconnect—in other words, on the exact location of the reconnection site along the vertical current sheet. This site does not remain at a fixed location, as in the Petschek model, but rather jumps discontinuously along the current sheet as different islands form (see Fig. 2). The islands further enhance and randomize the shear distribution as they move to one end of the sheet or the other and merge with previously reconnected field lines. Consequently, the reconnected field attains a seemingly chaotic shear pattern, which implies a large number of current sheets (Fig. 3).

Our simulations show that the width of the current structures in the reconnected region is comparable to the dissipation scale (~3 grid points, for our numerical scheme). Hence, they are true current sheets, much smaller than the gradients in the applied shear profile, and not simply fine-scale structures due to fine-scale boundary motions. The magnitude and quantity of current sheets will depend on factors such as the maximum prereconnection length of the vertical current sheet and the number of islands formed subsequently. We defer a detailed discussion of these issues to a subsequent paper.

It is important to recognize that RDCF does not require any special form or origin for the shear (e.g., footpoint motions). This process also would occur, for example, when a pretwisted emerging flux element reconnects with flux in the network. A

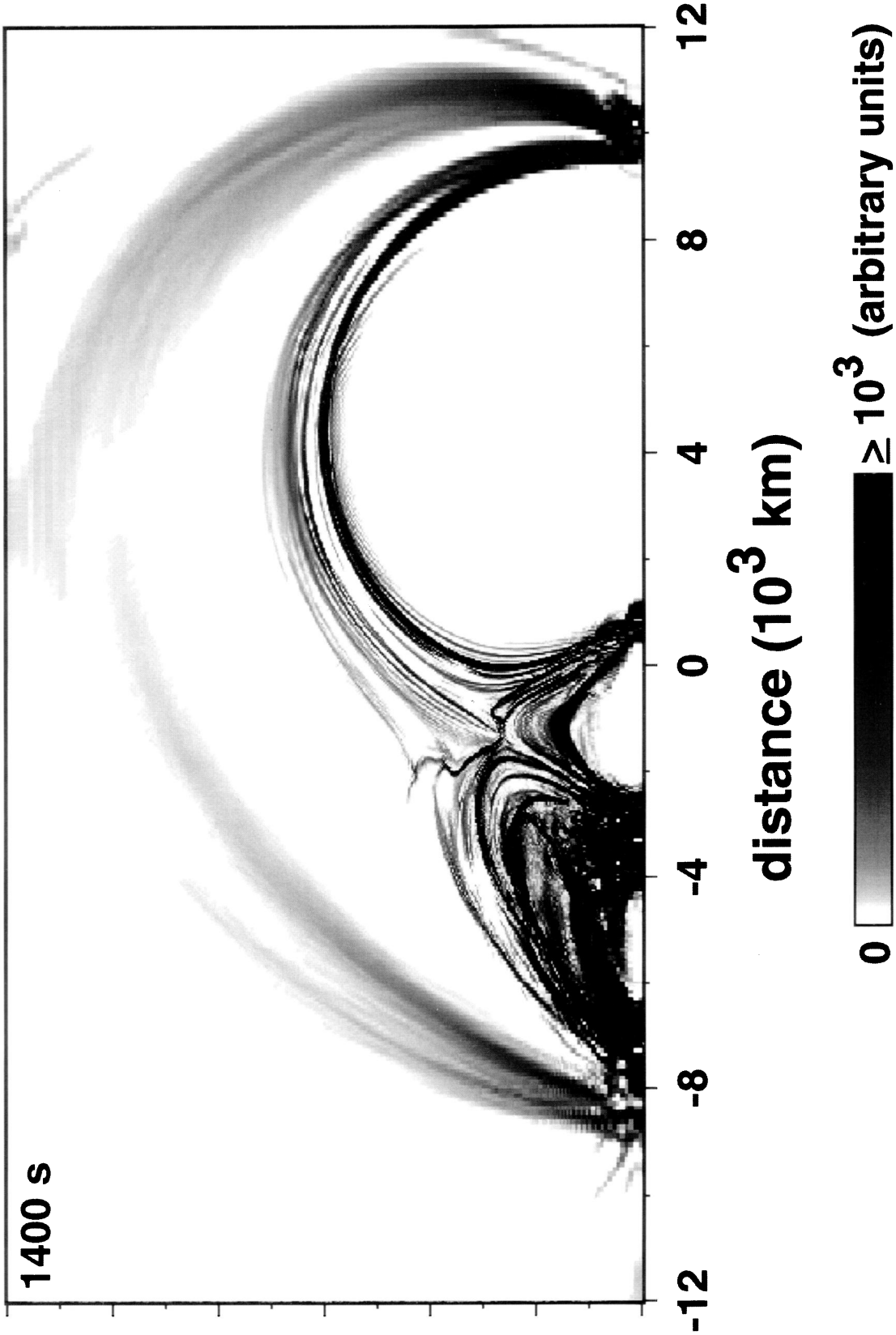

FIG. 3.—Electric current density ($j_x^2 + j_y^2$) during the relaxation phase (t = 1400 s). Note the band of filamentary currents over both arcades.

KARPEN, ANTIOCHOS, & DEVORE (see 460, L75)

similar process of field line randomization by reconnection has been observed in our recent three-dimensional study of magnetic flux tubes (Dahlburg, Antiochos, & Norton 1995). Given the ubiquitous presence of both sheared fields and multipolar regions, then, we expect RDCF to be a common phenomenon in the solar atmosphere. Note also that the only driven processes in the RDCF scenario are the formation and subsequent reconnection of the current sheet, which stems from the deformation of the initial X-point. Once the filamentary currents are created, they can heat the surrounding plasma through standard (much slower) resistive dissipation.

Our results have clear implications for DC models of coronal heating, which thus far have postulated the existence of the requisite fine structure in coronal loops without adequately explaining its origin. An attractive hypothesis is that coronal loops correspond to those flux tubes in a large arcade that interact with small bipolar regions near their footpoints. Reconnection between the larger and smaller flux systems leads to long-lived current sheets that decay slowly and yield the observed X-ray structures. Based on this scenario, we predict that small opposite-polarity regions should occur at the footpoints of X-ray loops, accompanied higher in the chromosphere and corona by plasma dynamics indicative of magnetic reconnection. High-resolution simultaneous observations in the optical, UV, and X-ray regimes, such as those to be obtained by *SOHO* and *TRACE*, will provide stringent tests of this hypothesis.

We can derive a rough estimate of the heating attributable to RDCF from the pre- and postreconnection total energies tracked during the simulation. The shear component of the total magnetic energy drops by $\sim 1.4 \times 10^{19}$ ergs cm^{-1} by the end of the run, from which is subtracted the change in total gravitational energy ($\sim 5 \times 10^{18}$ ergs cm^{-1}) and the maximum total kinetic energy in the computational plane ($\sim 2.2 \times 10^{18}$ ergs cm^{-1}) to obtain a thermal energy output of about 7×10^{18} ergs cm^{-1}. For the 1000 s characteristic timescale and 10^9 cm system size of our calculation, the resultant heat flux is approximately 7×10^6 ergs cm^{-2} s^{-1}, comparable to the heating requirements of a typical active region (Withbroe & Noyes 1977). We have begun a more rigorous assessment of the RDCF-associated heating, using a series of simulations with two significant modifications: increased spatial resolution, both to raise the Lundquist number above the present value of $\sim 3 \times 10^4$ and to allow scaling to the coronal regime; and much slower driving (by a factor of 10–100), for greater consistency with the observed photospheric flows.

We thank J. Klimchuk for helpful discussions. This work was supported by ONR and NASA's Space Physics Theory Program, by grants of computer time on the NCCS Cray C-98 at NASA/GSFC, and by a grant of HPC-MP time from the DoD Shared Resource Center on the CEWES C-916.

REFERENCES

Antiochos, S. K. 1987, ApJ, 312, 886
———. 1990, J. Italian Astron. Soc., 61, 369
Antiochos, S. K., Benka, S. G., Spicer, D. S., & Zalesak, S. T. 1994, Eos, 75, 273
Blake, M., & Sturrock, P. 1985, ApJ, 290, 359
Dahlburg, R. B., Antiochos, S. K., & Norton, D. 1995, Phys. Rev. Lett., submitted
Dere, K. P., Bartoe, J.-D. F., Brueckner, G. E., Ewing, J., & Lund, P. 1991, J. Geophys. Res., 96, 9399
DeVore, C. R. 1991, J. Comput. Phys., 92, 142
Falconer, D., Moore, R. L., Porter, J., & Shimizu, T. 1995, BAAS, 27, 976
Harvey, K. L., Nitta, N., Strong, K., & Tsuneta, S. 1994a, in X-Ray Solar Physics from *Yohkoh*, ed. Y. Uchida, T. Watanabe, K. Shibata, & H. Hudson (Tokyo: Universal Acad. Press), 21
Harvey, K. L., Strong, K., Nitta, N., & Tsuneta, S. 1994b, in Solar Active Region Evolution: Comparing Models with Observations, ed. K. S. Balasubramaniam & G. W. Simon (San Francisco: ASP), 377
Karpen, J. T., Antiochos, S. K., Dahlburg, R. B., & Spicer, D. S. 1993, ApJ, 403, 769
Karpen, J. T., Antiochos, S. K., & DeVore, C. R. 1991, ApJ, 382, 327
———. 1995, ApJ, 450, 422 (KAD)
Klimchuk, J. A. 1995, BAAS, 27, 966
Mikić, Z., Barnes, D. C., & Schnack, D. D. 1988, ApJ, 328, 830
Moses, J. D., et al. 1994, ApJ, 430, 913
Parker, E. N. 1963, ApJS, 8, 177
———. 1993, ApJ, 407, 342
Petschek, H. E. 1964, in AAS-NASA Symp. on Physics of Solar Flares, ed. W. N. Hess (Washington, DC: NASA), 425
Priest, E. R., Parnell, C. E., & Martin, S. F. 1994, ApJ, 427, 459
Rickard, G. J., & Priest, E. R. 1994, Sol. Phys., 151, 107
Rust, D. M. 1968, in IAU Symp. 35, Structure and Development of Solar Active Regions, ed. K. O. Kiepenheuer (Dordrecht: Reidel), 77
Shibata, K., Nozawa, S., & Matsumoto, R. 1992, PASJ, 44, 265
Sweet, P. A. 1958, in Electromagnetic Phenomena in Cosmic Physics, ed. B. Lehnert (New York: Cambridge Univ. Press), 123
Syrovatskii, S. I. 1971, Soviet Phys.–JETP, 33, 933
———. 1981, ARA&A, 19, 163
van Ballegooijen, A. A. 1986, ApJ, 311, 1001
Withbroe, G. L., & Noyes, R. W. 1977, ARA&A, 15, 363
Zwingmann, W., Schindler, K., & Birn, J. 1985, Sol. Phys., 99, 133